Talanta 161 (2016) 48–53

Contents lists available at ScienceDirect

Talanta

journal homepage: www.elsevier.com/locate/talanta

A label-free, PCR-free and signal-on electrochemical DNA biosensor for *Leishmania major* based on gold nanoleaves

M. Moradi [a], N. Sattarahmady [b,c], A. Rahi [b], G.R. Hatam [d,e], S.M. Rezayat Sorkhabadi [a,f], H. Heli [b,*]

[a] Pharmaceutical Sciences Branch, Islamic Azad University, Tehran, Iran
[b] Nanomedicine and Nanobiology Research Center, Shiraz University of Medical Sciences, Shiraz, Iran
[c] Department of Medical Physics, School of Medicine, Shiraz University of Medical Sciences, Shiraz, Iran
[d] Basic Sciences in Infectious Diseases Research Center, Shiraz University of Medical Sciences, Shiraz, Iran
[e] Department of Parasitology and Mycology, School of Medicine, Shiraz University of Medical Sciences, Shiraz, Iran
[f] Department of Pharmacology, Faculty of Medicine, Tehran University of Medical Sciences, Tehran, Iran

ARTICLE INFO

Article history:
Received 4 June 2016
Received in revised form
6 August 2016
Accepted 8 August 2016
Available online 9 August 2016

Keywords:
Leishmaniasis
DNA biosensor
Genosensor
Gold nanoleaves

ABSTRACT

Detection of leishmaniasis is important in clinical diagnoses. In the present study, identification of *Leishmania* parasites was performed by a label-free, PCR-free and signal-on ultrasensitive electrochemical DNA biosensor. Gold nanoleaves were firstly electrodeposited by an electrodeposition method using spermidine as a shape directing agent. The biosensor was fabricated by immobilization of a *Leishmania major* specific DNA probe onto gold nanoleaves, and methylene blue was employed as a marker. Hybridization of the complementary single stranded DNA sequence with the biosensor under the selected conditions was then investigated. The biosensor could detect a synthetic DNA target in a range of 1.0×10^{-10} to 1.0×10^{-19} mol L^{-1} with a limit of detection of 1.8×10^{-20} mol L^{-1}, and genomic DNA in a range of 0.5–20 ng μL^{-1} with a limit of detection of 0.07 ng μL^{-1}. The biosensor could distinguish *Leishmania major* from a non-complementary-sequence oligonucleotide and the *tropica* species with a high selectivity. The biosensor was applicable to detect *Leishmania major* in patient samples.

1. Introduction

Leishmania major is a species of protozoa found in the genus leishmania, and is associated with the disease zoonotic cutaneous leishmaniasis [1]. It is an intracellular pathogen which infects the macrophages and dendritic cells of the immune system [2]. The main form of transmission is through the sand fly vector (*Phlebotomus* species). However, transmission does not often occur in utero during blood transfusions or through interpersonal contact [3]. The incidence rate of cutaneous leishmaniasis is estimated to be between 1 and 1.5 million cases in a year. The disease is endemic in 88 countries of 5 continents with a total of 350 million people at risk [4]. *Leishmania major* is recognized as causing the majority of cases of cutaneous leishmaniasis across the Middle East, Northern Africa, and some areas of China and India.

Laboratory diagnosis of leishmaniasis can be made by the following manners: i) demonstration of the parasite in tissues of relevance by light microscopic examination of the stained specimen, in vitro culture, or animal inoculation; ii) detection of parasite DNA in tissue samples; or iii) immune diagnosis by detection of parasite antigen in the tissue, blood, or urine samples by detection of non-specific or specific antileishmanial antibodies (immunoglobulin), or by assay for leishmania-specific cell-mediated immunity [5]. The sensitivity of the tissue examination, except in the case of splenic aspirate, is low. Moreover, the procedure for obtaining the tissue specimen is traumatic and associated with considerable risk. Identification of amastigotes requires considerable expertize and training, and is subject to the ability of the observer [6]. Besides, parasite culture is expensive and time consuming, and requires expertize and costly equipments, severely restricting its use in routine clinical practice. The most common ways of diagnosing leishmaniasis is to identify amastigotes in a Wright-Giemsa-stained touch preparation or through isolation of the parasites in culture [7]. Due to the limitations inherent in techniques used for detection of parasites, new approaches to the detection of parasites, such as DNA hybridization, have been attempted since the early 1980s. Although these methods had a considerable sensitivity and several attempts have been made in this regard, it is still important to develop effective methods for

* Corresponding author.
E-mail addresses: hheli7@yahoo.com, heli@sums.ac.ir (H. Heli).

http://dx.doi.org/10.1016/j.talanta.2016.08.030
0039-9140/

the detection of *Leishmania major* [8].

Sensors and biosensors based on nanomaterials have been attracting increased attention due to their advantages such as low cost, simple design, small dimensions, and low power requirements [9–16]. Researches in this field would be beneficial to recognize the biotic origin, inheritance, growth, and evolution and create new methods for diagnosis, treatment, and prevention of human diseases [17,18]. Electrochemical DNA biosensors are able to offer simple, rapid, accurate and low-cost methods for testing of selected DNA sequences, and this has been the topic of considerable interest to many researchers [9,19–21].

In the present study, gold nanoleaves were electrodeposited in the presence of spermidine as shape directing agent. The nanoleaves were then employed to immobilize a specific single-stranded DNA (ssDNA) probe for *Leishmania major*, and fabrication of a signal-on electrochemical DNA biosensor without using PCR and any label. The biosensor can detect *Leishmania major* in patient samples.

2. Experimental section

2.1. Materials

All chemicals were of analytical grade from Scharlau (Spain) or Sigma (USA) and were used without further purification. All solutions were prepared by redistilled water. A probe oligonucleotide (*p*-DNA) was designed based on the genomic sequence of *Leishmania major*. p-DNA, a complementary-sequence oligonucleotide (target oligonucleotide, t-DNA) and a non-complementary-sequence oligonucleotide (non-target oligonucleotide, n-DNA) were purchased from Takapouzist Co. (Iran). The oligonucleotide sequences are as follows:

p-DNA sequence:

5′-SH-$(CH_2)_6$-TTTTTTTTTT-AACCCACTAAAGCGTCACCCAACA-3′.

t-DNA sequence:

5′-TGTTGGGTGACGCTTTAGTGGGTT-3′.

n-DNA sequence:

5′-AAACCAAAATGATCACCCCCATGC-3′.

The oligonucleotide stock solutions were prepared with 20 mmol L^{-1} Tris-HCl buffer, pH 7.4 solution (Tris) and kept frozen.

2.2. Electrodeposition of gold nanoleaves

Gold nanoleaves were electrodeposited on a polycrystalline gold disk (Au, 2 mm of diameter) electrode. The Au electrode was hand polished on a polishing microcloth by 50 nm-sized alumina powder lubricated by water to attain a mirror-like surface. The electrode was further electropolished by immersion in a 0.5 mol L^{-1} H_2SO_4 solution and applying the potential in the range of cathodic to anodic edges of the electrolyte stability in a regime of cyclic voltammetry for 20 consecutive cycles. Upon this pretreatment, a clean and stable gold surface was attained. The electrode was then transferred to a solution of 20 mmol L^{-1} $HAuCl_4$ + 0.5 mol L^{-1} H_2SO_4 + 150 mmol L^{-1} spermidine. Electrodeposition was performed at 0.0 V (vs. Ag/AgCl, 3 mol L^{-1} KCl) for duration of 300 s to obtain gold nanoleaves coated Au (GNL/Au) electrode. GNL/Au electrode was then rinsed thoroughly with redistilled water and dried at ambient temperature.

2.3. Physicochemical characterizations

Field emission scanning electron microscopy (FESEM) was performed using a Zeiss, Sigma-IGMA/VP (Germany) equipped with energy dispersive X-ray spectroscopy (EDS) capability.

2.4. Electrochemical measurements

Electrochemical measurements were performed in a conventional three-electrode cell powered by a μ-Autolab potentiostat/galvanostat run by a computer through GPES 4.9 software. An Ag/AgCl, 3 mol L^{-1} KCl, and a platinum rod were used as the reference and counter electrodes, respectively.

The real surface area of the GNL/Au electrode was measured electrochemically. The electrode was transferred to a solution of 0.5 mol L^{-1} KCl + 0.5 mmol L^{-1} $K_4[Fe(CN)_6]$ and cyclic voltammograms at different potential sweep rates were measured. Using the Randles-Sevcik equation [22] and the value of 7.60×10^{-6} cm s^{-1} for the diffusion coefficient of $[Fe(CN)_6]_4^-$ [23], the real surface area of the GNL/Au electrode was obtained.

Electrochemical detection of the DNA hybridization was performed in a 10 mL solution of Tris by differential pulse voltammetry for the reduction peak of bond methylene blue (MB). For differential pulse voltammetry, a pulse width of 25 mV, a pulse time of 50 ms, and a scan rate of 10 mV s^{-1} were employed. The concentrations of t-DNA solutions were quantified as the MB reduction peak currents.

2.5. Immobilization of p-DNA

Immobilization of p-DNA was performed by dropping 10 μL of 10 μmol L^{-1} p-DNA solution on the Au or GNL/Au electrode surfaces and remained intact at 4 °C for 8 h [24]. The electrodes were then rinsed thoroughly with Tris to remove unabsorbed p-DNA. Then, the electrodes were further treated with 10 μL 1.0 mmol L^{-1} 6-mercapto-1-hexanol for 30 min. The resultant electrodes were denoted as p-DNA-Au and the biosensor (p-DNA-GNL/Au).

2.6. Hybridization with t-DNA

The hybridization process was performed by dropping 10 μL of Tris containing various concentrations of t-DNA on the p-DNA-Au or p-DNA-GNL/Au electrode surfaces for 60 min at 37 °C [24]. During this procedure, a small vial was tightly fit on the electrodes' body to prevent quick evaporation of the droplet. Then, the electrodes were rinsed with Tris to remove the un-hybridized t-DNA, and then it was incubated in a solution containing Tris + 20 μmol L^{-1} MB for 5 min at room temperature [24]. Finally, the electrodes were rinsed with Tris to remove the physically adsorbed MB.

2.7. Parasite culture and genomic DNA extraction

The cryopreserved *Leishmania major* (MRHO/IR/75/ER) and *Leishmania tropica* (MHOM/IR/02/Mash10) were received from Tehran University of Medical Sciences, Tehran, Iran, reactivated, and cultivated in RPMI 1640 medium supplemented with 10% (v/v) heat-inactivated fetal bovine serum (Gibco) and 1% pen-strep (Sigma) at 24 °C. The promastigotes were counted daily in a Neubauer chamber until the concentration of 1×10^7 mL^{-1} parasites. Approximately, 10^7 phase promastigotes of isolates were harvested from the culture by centrifugation. The pellets were washed 3–4 times with chilled 50 mmol L^{-1} phosphate buffer saline (pH 7.0% and 0.7% NaCl) and suspended in 750 mL of NET buffer (5 mol L^{-1} NaCl, 0.5 mol L^{-1} EDTA, 1 mol L^{-1} Tris buffer, pH 8.0). The cells were lysed with Proteinase K (100 mg mL^{-1}) and 1% sodium dodecyl sulfate for 3–4 h at 56 °C. Total DNA was extracted by the YTA Genomic DNA extraction mini kit (Yekta Tajhiz Azma, Iran) following the manufacturer's instructions, and DNA was eluted in 100–150 μL of elution buffer. The parasitic DNA concentration was determined by a Thermo Scientific NanoDrop 2000c (USA), and was then diluted.

2.8. Genomic DNA extraction from human samples and PCR

Ten human biopsy specimens with cutaneous leishmaniasis were collected after sterilization of the lesion area on the slides, stained by Giemsa and microscopically characterized. Parasite DNA was extracted from 100 to 200 μL of the infected blood samples by the YTA Genomic DNA extraction Mini kit (Yekta Tajhiz Azma, Iran) following the manufacturer's instructions, and DNA was eluted in 100–150 μL of the elution buffer.

PCR followed by gel electrophoreses were performed to identify *Leishmania major* and *Leishmania tropica* in the human samples with cutaneous leishmaniasis. PCR primers were based on the non-protein coding region (AB678349.1) of *Leishmania major* minicircle kDNA (Iranian Standard strain MCAN/IR/97/LON490, isolate: IranJWmaj) [25], and purchased from Sinaclon, Iran. The YTA kit for tissue was employed.

3. Results and discussion

Fig. 1A-D shows FESEM images of the electrodeposited gold samples with different magnifications. At low magnifications, the gold sample resembles the tree leaves including midribs, veins, and laminas. At high magnification, the sample includes many adhered nanoparticles of 50–100 nm dimensions. EDS of the sample is presented in Fig. 1E confirms the purity of the gold nanoleaves. The special gold nanostructure synthesized here provides a suitable substrate to immobilize p-DNA, and can even promote the hybridization efficiency [26]. The real surface area of the gold nanoleaves was obtained as 0.67 cm^{-2}, while the

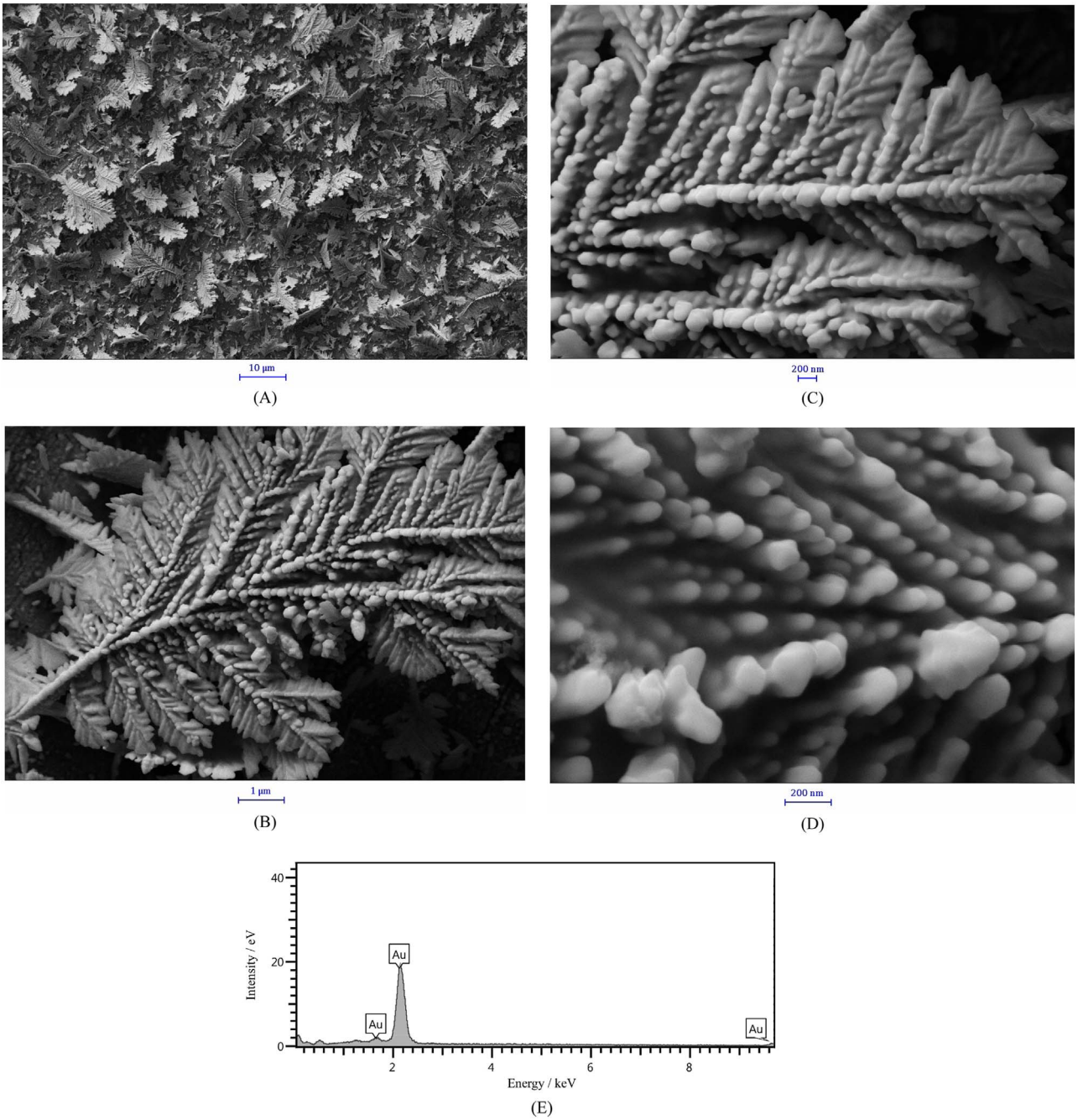

Fig. 1. FESEM images (A-D) and EDS (E) of the gold nanoleaves.

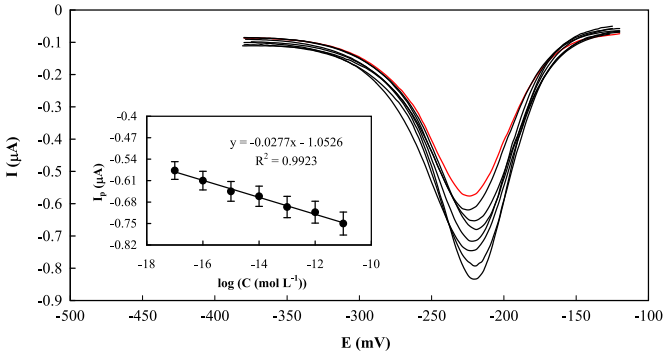

Fig. 2. DPVs of MB interacting with the p-DNA-Au electrode after hybridization with different concentrations of t-DNA of 1.0×10^{-17}, 1.0×10^{-16}, 1.0×10^{-15}, 1.0×10^{-14}, 1.0×10^{-13}, 1.0×10^{-12}, and 1.0×10^{-11} mol L^{-1}. The red curve is for the absence of t-DNA. Inset: the corresponding calibration curve. (For interpretation of the references to color in this figure legend, the reader is referred to the web version of this article.)

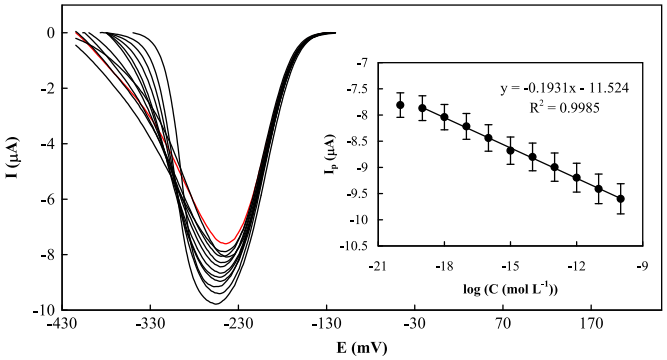

Fig. 3. DPVs of MB while interacted with the biosensor before and after hybridization with different concentrations of t-DNA of 1.0×10^{-19}, 1.0×10^{-18}, 1.0×10^{-17}, 1.0×10^{-16}, 1.0×10^{-15}, 1.0×10^{-14}, 1.0×10^{-13}, 1.0×10^{-12}, 1.0×10^{-11}, and 1.0×10^{-10} mol L^{-1}. The red curve is for the absence of t-DNA. Inset: the corresponding calibration curve. (For interpretation of the references to color in this figure legend, the reader is referred to the web version of this article.)

geometric surface area was 0.0314 cm^{-2}, indicating a roughness factor of 21.4. This indicates that GNL/Au electrode provides a large real surface area to immobilize a high surface concentration of p-DNA. During the electrodeposition of gold nanoleaves, gold atoms or clusters are initially and rapidly formed. Then, promoted nucleation of gold by the surface of Au electrode is followed [27]. On the other hand, spermidine, as a shape-directing agent and also as a poly-amine, is adsorbed on the (1 1 1) plane surface of the nuclei through a donation/back-donation mechanism of charge [28]. The spermidine adsorption process can lead to formation of an amine layer which bears positive charge (due to the acidic entity of the solution), and it causes further electrostatic adsorption of $AuCl_4^-$ ions and preferential growth of gold along the (1 1 1) directions by the diffusion-limited aggregation mechanism [29].

Fig. 2 shows differential pulse voltammograms (DPVs) of MB interacting with the p-DNA-Au electrode after hybridization with different concentrations of t-DNA. After hybridization, the peak current increased. This indicates the interaction of MB with both p-DNA and the resultant double stranded DNA (dsDNA), with higher affinity to dsDNA. MB binds to both ssDNA and dsDNA through electrostatic interactions and intercalation [30]. Intercalation is the dominated mode of binding here, due to the low ionic strength of the MB solution. This behavior was also observed elsewhere [31–33]. The dependency of the peak current on the t-DNA concentration is shown in the inset of Fig. 2. The plot is linear with a regression equation of $y=-(0.0277\pm0.0008)x-(1.0526\pm0.0120)$ in the range of 1.0×10^{-11} to 1.0×10^{-17} mol L^{-1} of t-DNA with a limit of detection (LOD, as 3 SD/m [34], SD is the standard deviation of blank signal, and m is the slope of the calibration curve) of 3.29×10^{-18} mol L^{-1}.

Fig. 3 shows DPVs of MB while interacting with the biosensor before and after hybridization with different concentrations of t-DNA recorded in Tris. The peak current of MB using the biosensor without hybridization with t-DNA was the lowest, and increased upon hybridization. The dependency of the peak current on the t-DNA concentration is shown in the inset of Fig. 3. The plot is linear with a regression equation of $y=-(0.1931\pm0.0027)x-(11.524\pm0.0393)$ in the concentration range of 1.0×10^{-10} to 1.0×10^{-19} mol L^{-1} of t-DNA with a LOD of 1.8×10^{-20} mol L^{-1}. The LOD obtained here is better than those reported previously [32,33]. The GNL/Au electrode surface provided a high surface area and, therefore, a high surface concentration of p-DNA and a dense probe layer was attained. Simultaneously, GNL/Au electrode surface may increase the deflection angle between p-DNA strands, alter their interactions, and cause appropriate orientations [35,36]. Therefore, the p-DNA layer was more accessible for t-DNA [37] to hybridize with an enhanced kinetics. On the other hand, the diffusion regime of MB during binding to p-DNA and dsDNA could also be change from linear to radial diffusion [38]. Scheme 1 represents the fabrication protocol of the biosensor and detection of t-DNA.

To detect the genomic DNA, the DNA genome was extracted from *Leishmania major* and the DNA concentrations in the extracted samples were determined. Then, solutions of the genome with different concentrations were prepared. The samples were placed in hot water of 90 °C for 10 min to de-hybridize the strands. After that, DPVs of MB while interacting with the biosensor, before and after hybridization with different concentrations of genomic target, were recorded. Fig. 4 shows these DPVs, and the corresponding calibration curve is presented in the inset. Based on these results, the genome of *Leishmania major* can be determined in a linear concentration range of 0.5–20 ng μL^{-1} with a LOD of 0.07 ng μL^{-1}. The LOD obtained here is lower than that reported previously [32].

In order to inspect the selectivity of the biosensor, a n-DNA sequence of 1.0×10^{-14} mol L^{-1} and the genome of *Leishmania tropica* were evaluated as negative controls. DNA genome of *Leishmania tropica* was extracted and de-hybridized in hot water and the genome concentration of 25 ng μL^{-1} was analyzed by the biosensor. The results of the selectivity of the biosensor are presented in Fig. 5. The results indicated that for both the samples, the peak currents in DPVs changed slightly, compared to the biosensor. This indicates the selectivity of the biosensor which can discriminate *Leishmania major* from *Leishmania tropica*.

As to the investigation of the fabrication reproducibility of the biosensor, it was placed in the Piranha solution for 30 s and then re-fabricated (n=5). DPVs of the biosensor for the repeating fabrications are shown in Fig. 6. Based on these results, there was a slight change in the peak currents, and a relative standard deviation (RSD) of 6.1% was obtained for the reproducibility of the biosensor fabrication.

In order to evaluate the regeneration behavior of the biosensor, after its hybridization with 1.0×10^{-17} mol L^{-1} t-DNA, it was immersed in hot water of 90 °C for 5 min to de-hybridize the formed dsDNA. Then, the biosensor was re-hybridized with the same t-DNA concentration (n=5). Fig. 7 shows the obtained DPVs indicating a RSD of 7.8% for the regeneration of the biosensor.

To inspect the stability of the biosensor, DPVs for 1.0×10^{-14} mol L^{-1} t-DNA over 16 days were recorded, while the biosensor was stored in Tris in the refrigerator at 4 °C and measured in a day in the same conditions. The data is presented in Fig. 8. The peak current showed a decrement after the first day,

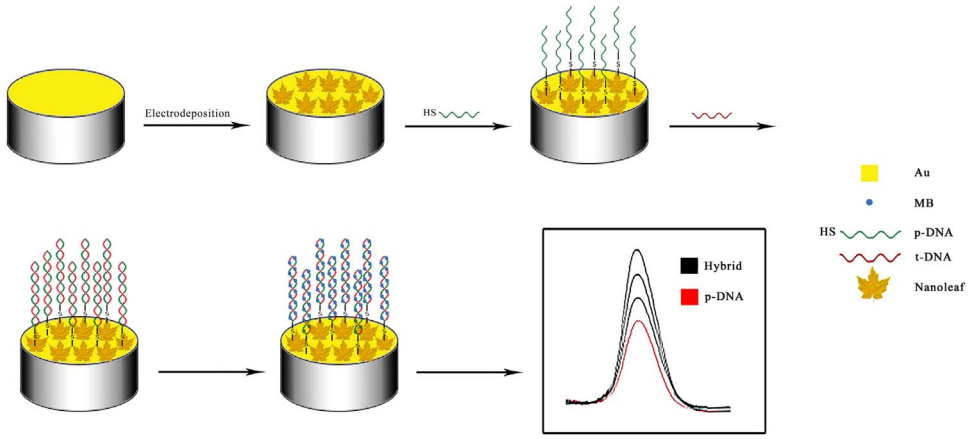

Scheme 1. Fabrication protocol of the biosensor and detection of t-DNA.

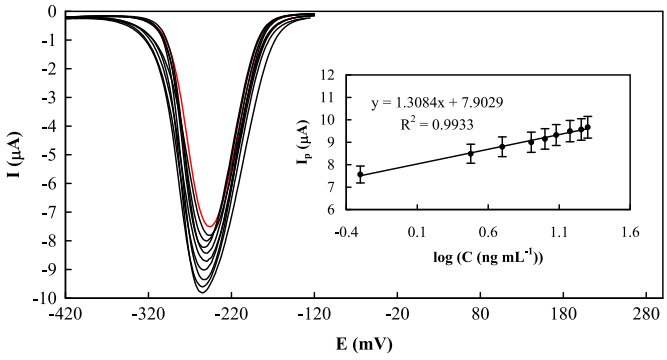

Fig. 4. DPVs of MB while interacted with the biosensor before and after hybridization with different concentrations of DNA genome of 0.5, 3, 5, 8, 10, 12, 15, 18, and 20 ng μL^{-1}. The red curve is for the absence of DNA genome. Inset: the corresponding calibration curve. (For interpretation of the references to color in this figure legend, the reader is referred to the web version of this article.)

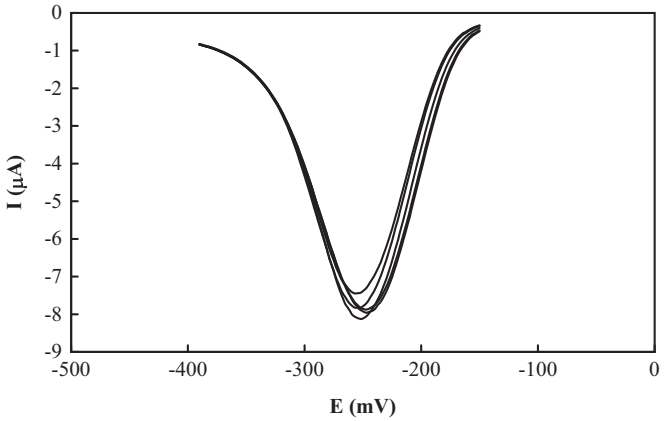

Fig. 6. DPVs of MB while interacted with the biosensor recorded after the repeating fabrications.

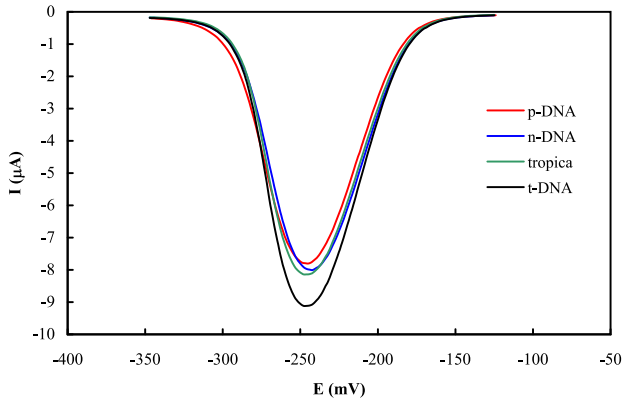

Fig. 5. DPVs of MB while interacted with the biosensor before (*p*-DNA), and after hybridization with the target oligonucleotide of 1.0×10^{-14} mol L^{-1} (*t*-DNA), a non-complementary sequence of 1.0×10^{-14} mol L^{-1} (*n*-DNA) and DNA genome of *Leishmania tropica* of 25 ng μL^{-1} (tropica).

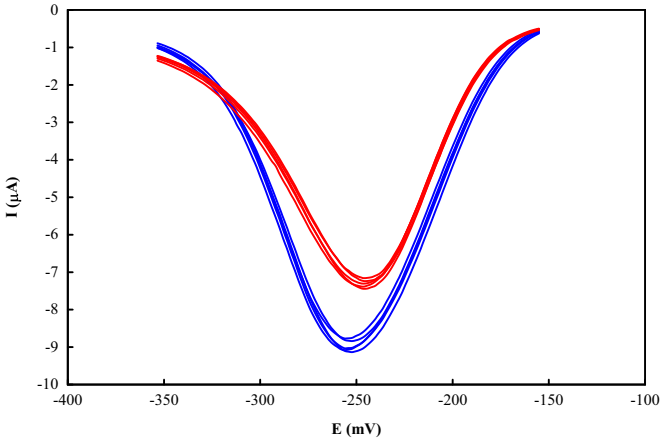

Fig. 7. DPVs of MB while interacted with the biosensor before (red curves) and after re-hybridization (n=5, blue curves) with 1.0×10^{-17} mol L^{-1} t-DNA. (For interpretation of the references to color in this figure legend, the reader is referred to the web version of this article.)

and it remained almost constant for about 13 days.

In order to apply the biosensor for diagnosis of cutaneous leishmaniasis in patients, human biopsy specimens with leishmaniasis were collected. The genomes were then extracted, and the presence of the *Leishmania major* was confirmed by PCR and gel electrophoresis. The concentration of DNA in the samples were then determined and a similar concentration of 5 ng μL^{-1} was prepared for all the samples. They were then de-hybridized and analyzed using the biosensor (Supplementary material S1). Increment in the peak currents in DPVs was recorded for theses samples, and on the other hand, the value of the limit of quantitation of the biosensor (LOQ, 10 SD/m [34], n=10) was measured. It was found that the increments in the peak currents for the samples containing *Leishmania major* were meaningfully higher than LOQ of the biosensor. Therefore, this label-free, PCR-free and signal-on biosensor had a capability of *Leishmania major* detection

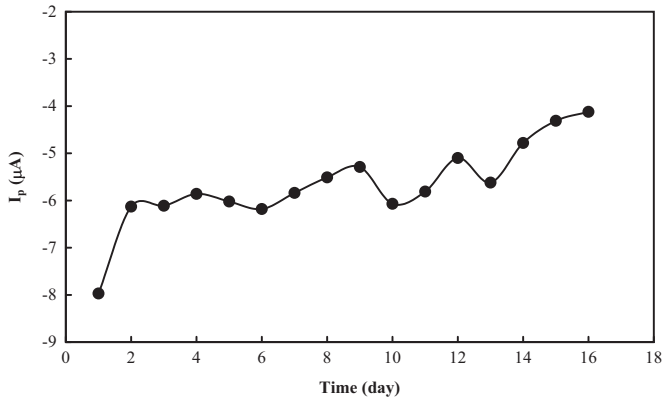

Fig. 8. Variation in the DPV peak currents of MB while interacted with the biosensor after hybridization with 1.0×10^{-14} mol L^{-1} t-DNA over 16 days.

in the samples from patients.

4. Conclusion

A simple green electrodeposition method was developed for the synthesis of gold nanoleaves at a surface using the biogenic polyamine spermidine. The proposed method is expandable for the synthesis of other nanostructures of gold with different shapes and sizes, or to the synthesis of other noble metal nanostructures.

- The nanoleaves provided a unique surface for the immobilization of a *Leishmania*-specific sequence with a high surface concentration to fabricate a DNA biosensor.
- The biosensor was applied for the detection of complementary sequence and extracted genome with a high sensitivity.
- The biosensor is label-free, PCR-free and signal-on and was applied to detect cutaneous leishmaniasis.

Acknowledgments

We would also like to thank the Research Council of Shiraz University of Medical Sciences and the Iran National Science Foundation (INSF) for supporting this research, and Prof. A. Khamesipour for his valuable assistances.

Appendix A. Supporting information

Supplementary data associated with this article can be found in the online version at doi:10.1016/j.talanta.2016.08.030.

References

[1] R. Lainson, J. Shaw, W. Peters, R. Killick-Kendrick, The Leishmaniases in Biology and Medicine, Academic Press, London, 1987.
[2] P. Desjeux, Leishmaniasis: current situation and new perspectives, Comp. Immunol. Microbiol. Infect. Dis. 27 (2004) 305–318.
[3] S. Sundar, M. Rai, Laboratory diagnosis of visceral leishmaniasis, Clin. Diagn. Lab. Immunol. 9 (2002) 951–958.
[4] F. Chappuis, S. Sundar, A. Hailu, H. Ghalib, S. Rijal, R.W. Peeling, J. Alvar, M. Boelaert, Visceral leishmaniasis: what are the needs for diagnosis, treatment and control? Nat. Rev. Microbiol. 5 (2007) 873–882.
[5] P.D. Marsden, T.C. Jones, Clinical Manifestations, Diagnosis and Treatment of Leishmaniasis, Elsevier Science Publishers, Amsterdam, 1985.
[6] L.F. Schur, R.L. Jacobson, Leishmaniasis in Biology and Medicine, Academic Press, New York, 2005.
[7] S. Gatti, M. Gramegna, C. Klersy, S. Madama, A. Bruno, R. Maserati, A. M. Bernuzzi, C. Cevini, M. Scaglia, Diagnosis of visceral leishmaniasis: the sensitivities and specificities of traditional methods and a nested PCR assay, Ann. Trop. Med. Parasitol. 98 (2004) 667–676.
[8] R. Reithinger, J.C. Dujardin, Molecular diagnosis of leishmaniasis: current status and future applications, J. Clin. Microbiol. 45 (2007) 21–25.
[9] T.G. Drummond, M.G. Hill, J.K. Barton, Electrochemical DNA sensors, Nat. Biotechnol. 21 (2003) 1192–1199.
[10] A. Rahi, K. Karimian, H. Heli, Nanostructured materials in electroanalysis of pharmaceuticals, Anal. Biochem. 497 (2016) 39–47.
[11] H. Heli, J. Pishahang, H. Barzegar Amiri, Synthesis of hexagonal CoAl-layered double hydroxide nanoshales/carbon nanotubes composite for the non-enzymatic detection of hydrogen peroxide, J. Electroanal. Chem. 768 (2016) 134–144.
[12] N. Sattarahmady, H. Heli, R. Dehdari Vais, A flower-like nickel oxide nanostructure: Synthesis and application for choline sensing, Talanta 119 (2014) 207–213.
[13] H. Heli, A. Rahi, Synthesis and applications of nanoflowers, Recent Pat. Nanotechnol. 10 (2016) 86–115.
[14] N. Sattarahmady, A. Movahedpour, H. Heli, G.R. Hatam, Gold nanoparticles-based biosensing of Leishmania major kDNA genome: visual and spectrophotometric detections, Sens. Actuators B 235 (2016) 723–731.
[15] N. Sattarahmady, Z. Kayani, H. Heli, Highly simple and visual colorimetric detection of Brucella melitensis genomic DNA in clinical samples based on gold nanoparticles, J. Iran. Chem. Soc. 12 (2015) 1569–1576.
[16] N. Sattarahmady, G.H. Tondro, M. Gholchin, H. Heli, Gold nanoparticles biosensor of Brucella spp. genomic DNA: visual and spectrophotometric detections, Biochem. Eng. J. 97 (2015) 1–7.
[17] H. Karadeniz, F. Kuralay, S. Abaci, A. Erdem, The recent electrochemical biosensor technologies for monitoring of nucleic acid hybridization, Curr. Anal. Chem 7 (2011) 63–70.
[18] M.I. Pividori, A. Merkoci, S. Alegret, Electrochemical genosensor design: immobilisation of oligonucleotides onto transducer surfaces and detection methods, Biosens. Bioelectron. 15 (2000) 291–303.
[19] H. Heli, N. Sattarahmady, G.R. Hatam, F. Reisi, R. Dehdari Vais, An electrochemical genosensor for Leishmania major detection based on dual effect of immobilization and electrocatalysis of cobalt-zinc ferrite quantum dots, Talanta 156–157 (2016) 172–179.
[20] A. Rahi, N. Sattarahmady, H. Heli, Label-free electrochemical aptasensing of the human prostate-specific antigen using gold nanospears, Talanta 156–157 (2016) 218–224.
[21] A. Rahi, N. Sattarahmady, H. Heli, An ultrasensitive electrochemical genosensor for Brucella based on palladium nanoparticles, Anal. Biochem. 510 (2016) 11–17.
[22] A.J. Bard, L.R. Faulkner, Electrochemical Methods, 2nd ed., John Wiley and Sons, New York, 2001.
[23] S.F. Wang, Q. Xu, Electrochemical parameters of ethamsylate at multi-walled carbon nanotube modified glassy carbon electrodes, Bioelectrochemistry 70 (2007) 296–300.
[24] A. Rahi, N. Sattarahmady, H. Heli, Zepto-molar electrochemical detection of Brucella genome based on gold nanoribbons covered by gold nanoblooms, Sci. Rep. 5 (2015) 18060.
[25] K. Pandey, B.D. Pandey, A.K. Mallik, J. Acharya, K. Kato, O. Kaneko, P.E. Ferreira, A new molecular surveillance system for leishmaniasis, Am. J. Trop. Med. Hyg. 90 (2014) 1082–1086.
[26] L. Soleymani, Z. Fang, E.H. Sargent, S.O. Kelley, Programming the detection limits of biosensors through controlled nanostructuring, Nat. Nanotechnol. 4 (2009) 844–848.
[27] J. Wang, G. Duan, Y. Li, G. Liu, Z. Dai, H. Zhang, W. Cai, An invisible template method toward gold regular arrays of nanoflowers by electrodeposition, Langmuir 29 (2013) 3512–3517.
[28] R.C. Hoft, M.J. Ford, A.M. McDonagh, M.B. Cortie, Adsorption of amine compounds on the Au (111) surface: A density functional study, J. Phys. Chem. 111 (2007) 13886–13891.
[29] J.T.A. Witten, L.M. Sander, Diffusion-limited aggregation, a kinetic critical phenomenon, Phys. Rev. Lett. 47 (1981) 1400–1405.
[30] E. Farjami, L. Clima, K.V. Gothelf, E.E. Ferapontova, DNA interactions with a methylene Blue redox indicator depend on the DNA length and are sequence specific, Analyst 135 (2010) 1443–1448.
[31] S. Radhakrishnan, C. Sumathi, V. Dharuman, J. Wilson, Polypyrrole nanotubes-polyaniline composite for DNA detection using methylene blue as intercalator, Anal. Methods 5 (2013) 1010–1015.
[32] M. Andreadou, E. Liandris, M. Gazouli, S. Taka, M. Antoniou, G. Theodoropoulos, I. Tachtsidis, N. Goutas, D. Vlachodimitropoulos, I. Kasampalidis, J. Ikonomopoulos, A novel non-amplification assay for the detection of Leishmania spp. in clinical samples using gold nanoparticles, J. Microbiol. Methods 96 (2014) 56–61.
[33] S. Mohan, P. Srivastava, S.N. Maheshwari, S. Sundar, R. Prakash, Nano structured nickel oxide based DNA biosensor for detection of visceral leishmaniasis (Kala-azar), Analyst 136 (2011) 2845–2851.
[34] J.C. Miller, J.N. Miller, Statistics for Analytical Chemistry, 4th ed., Ellis-Harwood, New York, 1994.
[35] H. Lord, S.O. Kelley, Nanomaterials for ultrasensitive electrochemical nucleic acids biosensing, J. Mater. Chem. 19 (2009) 3127–3134.
[36] H.D. Hill, J.E. Millstone, M.J. Banholzer, C.A. Mirkin, The role radius of curvature plays in thiolated oligonucleotide loading on gold nanoparticles, ACS Nano 3 (2009) 418–424.
[37] X. Bin, E.H. Sargent, S.O. Kelley, Nanostructuring of sensors determines the efficiency of biomolecular capture, Anal. Chem. 82 (2010) 5928–5931.
[38] M.A. Lapierre-Devlin, C.L. Asher, B.J. Taft, R. Gasparac, M.A. Roberts, S.O. Kelley, Amplified electrocatalysis at DNA-modified nanowires, Nano Lett. 5 (2005) 1051–1055.